

Implications of the cosmic infrared background excess for the cosmic star formation

Tan Wei-Wei & Yu Yun-Wei*

Institute of Astrophysics, Central China Normal University, Wuhan, China

Received 00, 0000; accepted 00, 0000; published online 00, 0000

By phenomenologically describing the high-redshift star formation history, i.e., $\dot{\rho}_*(z) \propto [(1+z)/4.5]^{-\alpha}$, and semi-analytically calculating the fractions of high-redshift Pop I/II and Pop III stars, we investigate the contributions from both high-redshift Pop I/II and Pop III stars to the observed near-infrared ($3 \mu\text{m} < \lambda < 5 \mu\text{m}$) excess in the cosmic infrared background emission. In order to account for the observational level of the near-infrared excess, the power-law index α of the assumed star formation history is constrained to within the range of $0 \lesssim \alpha \lesssim 1$. Such a constraint is obtained under the condition that the viral temperature of dark matter halos belongs to the range of $500 \text{ K} \leq T_{\text{vir}} \leq 10^4 \text{ K}$.

infrared background, star formation, dark matter

PACS number(s): 98.70.Vc; 98.62.Ai; 95.35+d

Citation: Tan Wei-Wei & Yu Yun-Wei. Implications of the cosmic infrared background excess for the cosmic star formation.

1 Introduction

In recent years, the cosmic star formation history (CSFH) is of more and more interest in both astrophysical and cosmological studies, especially the early universe where direct detections are difficult and scarce. As representative objects in the early universe, the first generation stars, commonly called Population III (hereafter Pop III) stars, would play a key role in the early evolution of the cosmic structure. Pop III stars are thought to originate from primordial metal-free gas at redshifts exceeding $z \sim 10$ and precede the normal metal-enriched stellar populations (see References [1–3] for reviews of Pop III stars). Direct observations of Pop III stars with current telescopes are impossible due to their high redshifts, although these stars are very massive and luminous. Alternatively, Pop III stars are expected to have left a great amount of diffuse radiation in the universe, which is shifted today into the infrared wavelength. For instance, for a photon at Lyman- α limit with $\lambda_s = 912 \text{ \AA}$ emitted from $z = 20$, its wavelength to be observed will be redshifted to $\lambda_r = \lambda_s(1+z) = 1.9 \mu\text{m}$. Therefore, a significant near-infrared

component from Pop III stars is expected to be present in the cosmic infrared background (CIB).

In the aspect of observation, a substantial near-infrared excess over the net fluxes produced by galaxies has been indeed inferred from the measurements of CIB anisotropies with COBE/DIRBE [4], Deep Spitzer Infrared Array Camera (IRAC) [5,6], Infrared Telescope in Space (IRTS) [7], and Hubble Ultra Deep Field (HUDF) [8]. The commonly known bolometric flux of such near infrared background excess (NIRBE) reads $F_{\text{excess}}^{\text{obs}} = (2.9 \pm 1.3) \times 10^{-5} \text{ erg s}^{-1} \text{ cm}^{-2} \text{ sr}^{-1}$ [9]. However, a more recent analysis by [8, 10] claimed that the flux of the NIRBE within the wavelength range of $3 \mu\text{m} < \lambda < 5 \mu\text{m}$ could be ten times smaller as

$$F_{\text{excess}}^{\text{obs}} \approx 1 \times 10^{-6} \text{ erg s}^{-1} \text{ cm}^{-2} \text{ sr}^{-1}, \quad (1)$$

because much of the previously estimated excess could be due to inaccurate zodiacal light modeling [11].

Therefore, in this paper, we would use the observed NIRBE to constrain the formation history of Pop III stars as well as the properties of the first collapsing dark matter halos hosting such stars. These halos may be too faint to be observed with the current telescopes. Different from some previous research studies, in our considerations, we also take

*Corresponding author (email: yuyw@phy.ccnu.edu.cn)

into account the contribution to the NIRBE from normal Pop I/II stars at high redshifts, because in the process of derivation of the NIRBE flux, only the emission from the galaxies at relatively low redshifts $z \lesssim 10$ was subtracted [8]. In the next section, we would present our theoretical consideration of the formation rates of Pop III and Pop I/II stars, where several free parameters are introduced. In section III, by confronting the theoretical NIRBE with the observational NIRBE, we constrain the model parameters. Finally, a summary and discussion are given in the last section.

2 Star formation rates

In principle, the formation rate of Pop III stars can be theoretically derived in the hierarchical formation model (e.g., [12, 13]), which however involves many complicated astrophysical issues. Therefore, in order to decrease the model uncertainties and utilize some observational information, we here give a phenomenological description for the CSFH and a semi-analytical calculation for the fraction of Pop III stars.

2.1 Cosmic star formation history

Following a series of measurements of star formation rate density, especially the complication of Hopkins & Beacom [14], a consensus on the CSFH now emerges up to redshift $z \sim 3.5$, which includes a steady increase of star formation from $z = 0$ to $z = 1$, and a following plateau up to $z \sim 3.5$. An empirical fitting can be written as

$$\dot{\rho}_*(z) \propto \begin{cases} (1+z)^{3.44}, & \text{for } z \leq 0.97, \\ (1+z)^0, & \text{for } 0.97 \leq z \leq 3.5, \end{cases} \quad (2)$$

with a local rate density $\dot{\rho}_*(0) = 0.02 M_\odot \text{ yr}^{-1} \text{ Mpc}^{-3}$. In contrast, for higher redshifts, the situation is still ambiguous. It could continue to plateau, drop off, or even increase, e.g., as considered in [15]. Therefore, we here simply introduce a new free parameter α to parameterize the high-redshift CSFH as follows

$$\dot{\rho}_*(z) \propto (1+z)^{-\alpha}, \text{ for } z \gtrsim 3.5. \quad (3)$$

The power-law assumption adopted above is motivated by the shapes of the history at $z \lesssim 3.5$ (see equation 2) and also implied by some preliminary measurements of the high-redshift star formation rates through Lyman break galaxies [16] and through gamma-ray bursts as well as their host galaxies [17–20].

As a phenomenological consideration, we further assume that the star formation rate density given by equation (3) has contained both the contributions from Pop I/II and Pop III stars.

2.2 Fraction of Pop III stars

In the hierarchical formation model, star formation takes place during the collapse and merging of dark matter halos. The formation of the halos hosting zero-metallicity Pop III

stars should satisfy two fundamental conditions: (i) The halos must be “freshly” formed through collapse of diffuse dark matter but not through merging of smaller halos. In these new halos, the stars are formed for the first time. (ii) The newly formed halos are not located in the wind radius, R_w , of old galaxies, because the intergalactic medium within R_w has been metal enriched by the galactic winds (i.e., feedback effect) [21–23]. Here the wind radius R_w is defined as the Sedov radius of the galactic wind, which is mainly determined by the total energy of all supernovae in the galaxy. For typical energy release per supernova $E_{SN} \sim 10^{52} \text{ erg}$ and typical mass of Pop III stars $M \sim 100 M_\odot$, we can have $R_w \sim 380 (m/10^{10} M_\odot)^{1/5} [(1+z)/10]^{-3/5} \text{ kpc}$.

For the first condition, following Furlanetto & Loeb [24], the fraction of matter that can collapse into “new” halos can be expressed by

$$f_{\text{new}}(z) \approx \int_{\infty}^z \frac{m_{\text{min}}^2}{\bar{\rho}} \frac{\delta_c(z')}{\sigma(m_{\text{min}})} n(m_{\text{min}}) \left| \frac{d}{dz'} \frac{\delta_c(z')}{\sigma(m_{\text{min}})} \right| dz', \quad (4)$$

where $\bar{\rho}$ is the mean cosmic density, $\delta_c(z)$ is the critical density for collapse, $\sigma(m)^2$ is the variance of the density field on the mass scale m , $n(m)$ is the Press & Schechter mass function [25], and m_{min} is the minimum halo mass. With a given virial temperature T_{vir} , the minimum halo mass can be estimated by equating the gravitational force of the halos to the opposing gas pressure [26]

$$m_{\text{min}}(z) \approx 10^8 M_\odot \left(\frac{\mu}{0.6} \right)^{-3/2} \left(\frac{T_{\text{vir}}}{10^4 \text{ K}} \right)^{3/2} \left(\frac{1+z}{10} \right)^{-3/2}, \quad (5)$$

where μ is the mean molecular weight, with $\mu = 0.6$ for ionized gas and $\mu = 1.22$ for neutral primordial gas. Here we choose $\mu = 1.22$ as the universe is mostly neutral at high redshifts.

For the second condition, the probability that a new halo lies within R_w of an existing galaxy can be approximated by [24]

$$p_e \approx 1 - \exp \left[-(1+B) \int_{m_{\text{min}}}^{\infty} \frac{m}{\bar{\rho}} \eta(m) n(m) dm \right], \quad (6)$$

where $\eta(m)$ is the ratio of the mass metal-enriched by galactic winds to the total mass of each galaxy. Following Furlanetto & Loeb [24], we have

$$\eta(m) \approx 27 K_w \left(\frac{m}{10^{10} M_\odot} \right)^{-2/5} \left(\frac{10}{1+z} \right)^{3/5}, \quad (7)$$

where the normalization factor $0 \leq K_w \leq 1/8$ accounts for many feedback factors (e.g., radiative losses from supernova shocks). A higher value of K_w represents stronger feedback effects. For the formation of Pop III stars, such feedback effect is a negative effect. The coefficient B appearing in Equation (6) gives the excess probability that two galaxies sit near each other, by considering that the collapsing halos are actually biased due to the existing halos and inclined to be near the existing halos. To be specific, $B \approx \zeta_{\text{mm}}(\bar{R}_w) b(m_{\text{min}}) \langle b(m) \rangle$, where $\zeta_{\text{mm}}(\bar{R}_w)$ (with \bar{R}_w to be

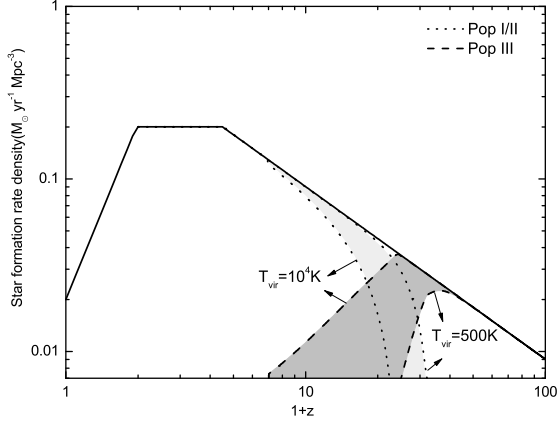


Figure 1 The CSFHs of Pop III stars (dashed lines), Pop I/II stars (dotted lines), and their sum (solid lines), where $\alpha = 1.0$ and $K_w = 0.02$ are taken. The shaded region represents the variation of the virial temperature from $T_{\text{vir}} = 500$ K to 10^4 K.

the average wind size in the comoving units) is the dark matter correlation function [27], $b(m)$ is the bias function [28], and the bracket $\langle \dots \rangle$ represents an average on the Press & Schechter mass function [29].

2.3 Formation rates of Pop III and I/II stars

Combining the two aspects addressed above, the formation rate density of Pop III stars as a function of z can be given by

$$\dot{\rho}_{\text{III}}(z) = \dot{\rho}_*(z) \left(\frac{df_{\text{new}}/dz}{df_{\text{coll}}/dz} \right) (1 - p_e), \quad (8)$$

where $f_{\text{coll}}(z)$ is the fraction of matter that can collapse into “all” of halos. For the Press & Schechter mass function, it reads [24]

$$f_{\text{coll}}(z) = \text{erfc} \left[\frac{\delta_c(z)}{\sqrt{2}\sigma(m_{\text{min}})} \right]. \quad (9)$$

Meanwhile, the formation rate density of Pop I/II stars can be obtained by subtracting the rate density of Pop III stars from the total star formation rate density

$$\dot{\rho}_{\text{I/II}}(z) = \dot{\rho}_*(z) - \dot{\rho}_{\text{III}}(z). \quad (10)$$

In the model described above, three free parameters remain: α , T_{vir} , and K_w . As theoretically considered, the value of T_{vir} is in principle determined by the cooling style of the halos. The radiative cooling through molecular hydrogen would lead to $T_{\text{vir}} \sim 500$ K [30, 31], while the atomic cooling gives $T_{\text{vir}} \sim 10^4$ K (e.g., [32, 33]). Hence the specific value of T_{vir} relies on the fraction of molecular hydrogen. For the temperature range of $500 \text{ K} \leq T_{\text{vir}} \leq 10^4 \text{ K}$, we present a numerical result of the CSFH in Figure 1, which indicates that: (i) the formation of Pop III stars would dominate the cosmic

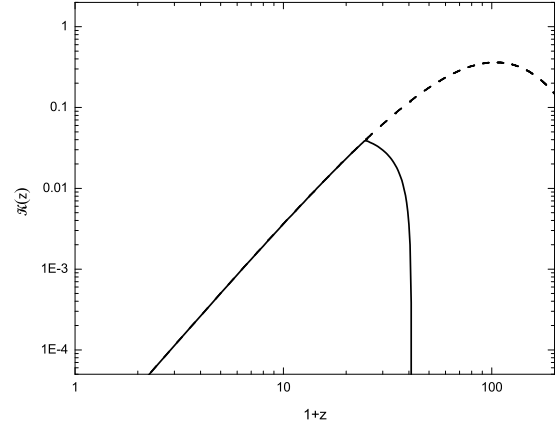


Figure 2 The dependence of the correction factor $\mathcal{K}(z)$ on redshift for stellar temperature $T = 10^5$ K (solid line), which peaks at $z_p = 24$ due to Ly- α absorption. The case without Ly- α absorption is also presented by the dashed line for comparison.

star formation for $z > (20 \sim 40)$, and (ii) higher virial temperature T_{vir} could extend the formation of Pop III stars to lower redshifts.

3 NIRBE emission

Instead of an elaborate fitting to observations, here we would use the observed bolometric flux of the NIRBE (Equation 1) to constrain the model parameters. In the following calculations, the contributions from Pop III stars and high-redshift Pop I/II stars are both taken into account.

3.1 Pop III stars

As massive, zero-metallicity stars, Pop III stars would radiate close to the Eddington limit $L_{\text{edd}} = (4\pi G m_p c / \sigma_T) M \simeq 1.3 \times 10^{38} (M/M_\odot) \text{ erg s}^{-1}$, where M is the stellar mass. Then the lifetime of Pop III stars can be estimated by $t_L \simeq \varepsilon M c^2 / L_{\text{edd}} \simeq 3.1 \times 10^6 \text{ yr}$, which is independent of the stellar masses, where $\varepsilon = 0.007$ is taken as a fiducial value. Here Pop III stars are not considered for significant mass loss during their lifetimes because of their zero metallicity. The black body effective temperature of Pop III stars can be estimated to $T_{\text{III}} \sim 10^5$ K with the Eddington luminosity and the theoretical Hertzsprung-Russell diagram of Pop III stars [34, 35].

At redshift z , the density of the energy radiated from Pop III stars can be expressed by

$$\mathcal{E}_{\text{III}}(z) \approx \varepsilon \dot{\rho}_{\text{III}}(z) c^2 t_H(z), \quad (11)$$

which is released within the duration of t_L , where $t_H(z) \approx (2/3)H(z)^{-1}$ is the Hubble timescale at that redshift. In the standard Λ -cold dark matter cosmology, the Hubble expansion rate reads $H(z) = H_0 \sqrt{(1+z)^3 \Omega_m + \Omega_\Lambda}$. Hereafter $H_0 = 71 \text{ km s}^{-1} \text{ Mpc}^{-1}$, $\Omega_\Lambda = 0.73$, and $\Omega_m = 0.27$ are taken. Therefore, the bolometric flux of the NIRBE contributed by

Pop III stars can be calculated by

$$F_{\text{excess}}^{\text{III}} = \frac{1}{4\pi} \int \mathcal{K}_{\text{III}}(z) \frac{\mathcal{E}_{\text{III}}(z)/t_L}{4\pi d_I(z)^2} dV_c(z), \quad (12)$$

where $\mathcal{K}_{\text{III}}(z)$ represents the fraction of energy that enters the near-infrared wavelength range of $3 \mu\text{m} < \lambda < 5 \mu\text{m}$, $d_I(z)$ and $dV_c(z)$ are luminosity distance and comoving volume element, respectively. To be specific, $d_I(z) = c(1+z) \int_0^z H^{-1}(z') dz'$ and $dV_c(z) = 4\pi d_c(z)^2 c H^{-1}(z) dz$ with $d_c(z) = d_I(z)/(1+z)$. By considering that $\Omega_\Lambda \ll \Omega_m(1+z)^3$ for high redshifts, we can simplify the above equation to

$$F_{\text{excess}}^{\text{III}} \approx \frac{c l_{\text{III}}}{6\pi H_0^2 \Omega_m} \int \frac{\mathcal{K}_{\text{III}}(z) \dot{\rho}_{\text{III}}(z)}{(1+z)^5} dz, \quad (13)$$

where Equation (11) is used and $l_{\text{III}} = L_{\text{Edd}}/M = 6.3 \times 10^4 \text{ erg s}^{-1} \text{ g}^{-1}$ represents the luminosity per unit stellar mass.

For a black body spectrum described by the Planck function $B_T(\lambda)$ for temperature T , the correction factor $\mathcal{K}(z)$ can be generally calculated by

$$\mathcal{K}(z) = \frac{\int_{\lambda_1/(1+z)}^{\lambda_2/(1+z)} B_T(\lambda) d\lambda}{\int_0^\infty B_T(\lambda) d\lambda} \quad (14)$$

with $\lambda_1 = 3 \mu\text{m}$ and $\lambda_2 = 5 \mu\text{m}$ [10]. However, as revealed by WMAP, the reionization of the universe completes at most as early as redshift ~ 10.5 , before which the universe is neutral [36]. Consequently, for stars at high redshifts, photons emitted from them with wavelengths shorter than the Ly- α wavelength (i.e., $\lambda_e \leq 1216 \text{ \AA}$) must be all absorbed by the diffuse neutral hydrogens (as the Gunn-Peterson trough in the spectra of high-redshift quasars). Therefore, the lower limit of the integral in the numerator of Equation (14) needs to be changed to $\max[\lambda_1/(1+z), 1216 \text{ \AA}]$. In the extreme, if $\lambda_2/(1+z) < 1216 \text{ \AA}$, then we have $\mathcal{K}(z) = 0$.

For Pop III stars with $T = 10^5 \text{ K}$, a numerical result of $\mathcal{K}_{\text{III}}(z)$ as a function of redshift is presented in Figure 2. As is shown, it firstly increases as $(1+z)^3$ up to $z_p = 3 \mu\text{m}/1216 \text{ \AA} - 1 = 24$, and then plunges to zero at $z_{\text{max}} = 5 \mu\text{m}/1216 \text{ \AA} - 1 = 40$. The peak value of $\mathcal{K}_{\text{III}}(z)$ at z_p can be analytically calculated by

$$\mathcal{K}_{\text{III}}(z_p) = \frac{2\pi h c^2}{\sigma T^4 \lambda_c^5} \frac{(1+z_p)^4 \Delta\lambda}{\exp[(1+z_p)hc/k_B T \lambda_c] - 1}, \quad (15)$$

where $\lambda_c = 4 \mu\text{m}$ and $\Delta\lambda = 2 \mu\text{m}$. Moreover, due to $(1+z_p) \ll 4k_B T \lambda_c / hc$, the peak value can be approximately expressed by

$$\mathcal{K}_{\text{III}}(z_p) \approx \frac{\pi c k_B \Delta\lambda}{\sigma \lambda_c^4} \frac{1}{T^3} (1+z_p)^3, \quad (16)$$

which is proportional to T^{-3} for $T > 2 \times 10^4 \text{ K}$.

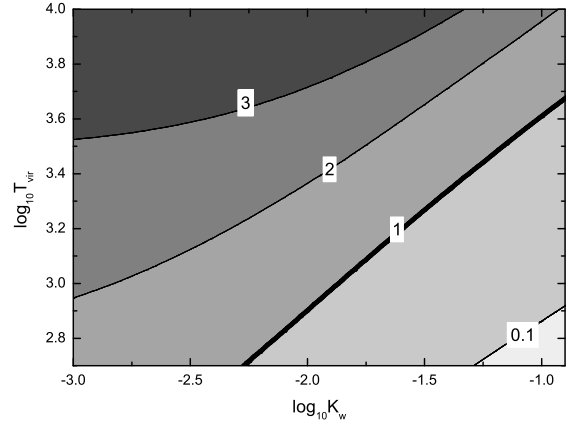


Figure 3 The distribution of the ratio $F_{\text{excess}}^{\text{III}}/F_{\text{excess}}^{\text{I/II}}$ in the $K_w - T_{\text{vir}}$ parameter space.

3.2 Pop I/II stars

Following Equation (13), the contribution to the NIRBE emission from high-redshift Pop I/II stars can be calculated by

$$\frac{dF_{\text{excess}}^{\text{I/II}}}{d\tilde{M}} = \frac{c l_{\text{I/II}}}{6\pi H_0^2 \Omega_m} \int \frac{\mathcal{K}_{\text{I/II}}(z) d\dot{\rho}_{\text{I/II}}(z)}{(1+z)^5 d\tilde{M}} dz, \quad (17)$$

where $\tilde{M} \equiv M/M_\odot$ is the dimensionless stellar mass. The lower limit of the above integral is set at $z \sim 10$ since the contributions from Pop I/II stars at relatively low redshift $z \lesssim 10$ have been subtracted from the excess emission [8]. The differential form is taken in Equation (17) due to the wide distribution of the mass of Pop I/II stars. So, different from Pop III stars, both the quantities $l_{\text{I/II}}$ and $\mathcal{K}_{\text{I/II}}(z)$ here should be treated as functions of stellar mass. Specifically, the empirical mass-luminosity relation for Pop I/II stars tells us $l_{\text{I/II}} \approx \tilde{M}^{2.5} (L_\odot/M_\odot)$. Meanwhile, we can estimate the stellar temperature by $T \sim 5000 \tilde{M}^{0.6} \text{ K}$ according to the Hertzsprung-Russel diagram of Pop I/II stars. For the Salpeter initial mass function, $\phi(\tilde{M}) \propto \tilde{M}^{-2.35}$, the differential star formation rate can be expressed by

$$\frac{d\dot{\rho}_{\text{I/II}}(z)}{d\tilde{M}} = A \dot{\rho}_{\text{I/II}}(z) \tilde{M} \phi(\tilde{M}), \quad (18)$$

where $A = \left[\int_{\tilde{M}_{\text{min}}}^{\tilde{M}_{\text{max}}} \tilde{M} \phi(\tilde{M}) d\tilde{M} \right]^{-1} = 0.17$ with $\tilde{M}_{\text{min}} = 0.1$ and $\tilde{M}_{\text{max}} = 100$. Then, we have

$$F_{\text{excess}}^{\text{I/II}} = \frac{Ac}{6\pi H_0^2 \Omega_m} \left(\frac{L_\odot}{M_\odot} \right) \times \int \tilde{M}^{1.15} \int \frac{\mathcal{K}_{\text{I/II}}(z) \dot{\rho}_{\text{I/II}}(z)}{(1+z)^5} dz d\tilde{M}. \quad (19)$$

In Figure 3, we plot the distribution of the ratio of $F_{\text{excess}}^{\text{III}}$ to $F_{\text{excess}}^{\text{I/II}}$ in the $K_w - T_{\text{vir}}$ parameter space¹, which indicates that the contribution to the NIRBE from high-redshift Pop I/II

¹ The dependence of this ratio on the parameter α is insensitive, because α influences the formation rates of Pop III and I/II stars in a same way.

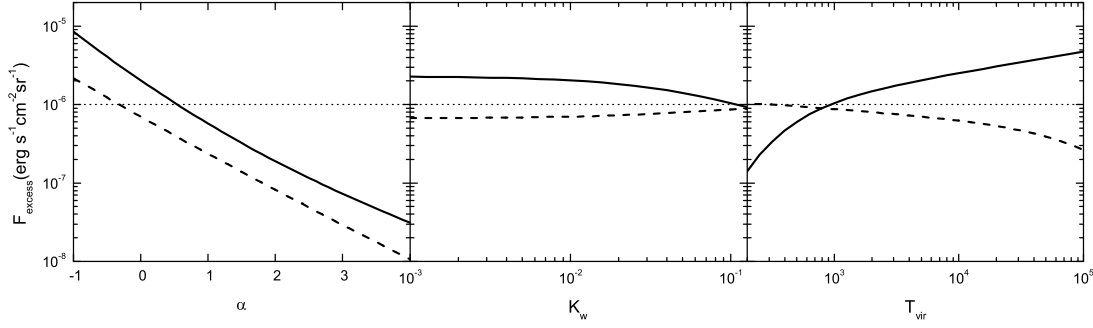


Figure 4 Dependence of F_{excess} on the free model parameters for Pop III stars (solid lines) and high-redshift Pop I/II stars (dashed lines), where the fiducial values of the parameters are taken to $T_{\text{vir}} = 5000$ K, $K_w = 0.01$, and $\alpha = 0$. The horizontal dotted line represents the observed flux of the NIRBE as $1 \times 10^{-6} \text{ erg s}^{-1} \text{ cm}^{-2} \text{ sr}^{-1}$.

stars could be much more significant than previously considered, especially for low T_{vir} and high K_w .

From Equation (19), we can see that the value of $F_{\text{excess}}^{\text{I/II}}$ could be mainly determined by the highest-mass stars having temperatures $T > 2 \times 10^4$ K. Therefore, following Equation (16), we can get

$$\frac{\mathcal{K}_{\text{I/II}}(z)}{\mathcal{K}_{\text{III}}(z)} \approx \left(\frac{T_{\text{I/II}}}{T_{\text{III}}} \right)^3 \approx \frac{\tilde{M}^{1.8}}{8000}, \quad (20)$$

where the peak redshift z_p is replaced by an arbitrary redshift z because the profiles of the functions $\mathcal{K}(z)$ are basically identical so long as $T > 2 \times 10^4$ K. For a more direct comparison with Pop III stars (Equation 13), we rewrite Equation (19) to

$$F_{\text{excess}}^{\text{I/II}} \approx \frac{c l'_{\text{I/II}}}{6\pi H_0^2 \Omega_m} \int \frac{\mathcal{K}_{\text{III}}(z) \dot{\rho}_{\text{I/II}}(z)}{(1+z)^5} dz, \quad (21)$$

where the equivalent luminosity per unit stellar mass reads

$$l'_{\text{I/II}} = A \left(\frac{L_\odot}{M_\odot} \right) \int \frac{\tilde{M}^{2.95}}{8000} d\tilde{M} = 850 \text{ erg s}^{-1} \text{ g}^{-1}, \quad (22)$$

which gives a ratio $l'_{\text{I/II}}/l_{\text{III}} = 0.014$. Therefore, if $\dot{\rho}_{\text{I/II}}$ is hundreds times higher than $\dot{\rho}_{\text{III}}$, the contribution to the NIRBE from high-redshift Pop I/II stars can exceeds that from Pop III stars. As exhibited in Figure 3, such a situation can arise with low T_{vir} and high K_w .

3.3 Constraining the CSFH

The dependence of the model-predicted NIRBE fluxes on the parameters T_{vir} , K_w , and α are shown in Figure 4 for both Pop III and I/II stars. As can be seen, the uncertainty of the NIRBE fluxes mainly comes from the uncertainties of α and T_{vir} , whereas the variation of K_w only slightly influences the value of F_{excess} .

Combining Equations (13) and (19), the model-predicted flux of the NIRBE emission contributed by both Pop III and high-redshift Pop I/II stars can be calculated by

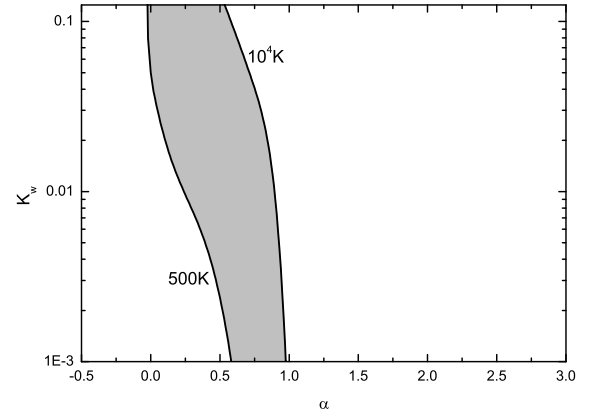


Figure 5 The parameter region where the model-predicted NIRBE flux can account for the observational one (shaded region). The two boundaries of the region corresponds to the virial temperatures of 500 K and 10^4 K, respectively.

$$F_{\text{excess}}^{\text{model}} = F_{\text{excess}}^{\text{III}} + F_{\text{excess}}^{\text{I/II}}. \quad (23)$$

As shown in Figure 5, by equating $F_{\text{excess}}^{\text{model}}$ to $F_{\text{excess}}^{\text{obs}}$, we find a tight constraint on the model parameters α as $0 \lesssim \alpha \lesssim 1$, where the other two model parameters are considered to $500 \text{ K} \leq T_{\text{vir}} \leq 10^4 \text{ K}$ and $K_w \leq 1/8$. This result indicates that the high-redshift CSFH could be very flat. On the other hand, specifically, lower virial temperature T_{vir} leads to lower formation rates of Pop III stars, and thus the total formation rate is required to be higher in order to have more Pop I/II stars to produce emission.

4 Summary and discussion

In view of the inaccessible direct observations of high-redshift stars, especially Pop III stars and their hosts, we propose an indirect method to study these high-redshift objects

by using the observed CIB emission, particularly, the NIRBE emission. In our model, the CSFH are described phenomenologically, in order to decrease the complexity of the model. Consequently, a strong constraint on the CSFH is found as $0 \lesssim \alpha \lesssim 1$, if the viral temperature of the halos satisfies $500 \text{ K} \leq T_{\text{vir}} \leq 10^4 \text{ K}$. Such a flat CSFH basically agrees with the star formation rates inferred from high-redshift gamma-ray bursts up to redshift $z \sim 8-9$ [18]. In contrast, for higher redshift (e.g., $z \sim 10$), a recent measurement by [37] claimed that the star formation rate could become much lower. These observations imply that the realistic CSFH may exhibit a behavior more complicated than a single power law. Anyway, on the other hand, the CSFH with $0 \lesssim \alpha \lesssim 1$ predicts sufficiently bright sources to reionize the universe to account for the optical depth of cosmic microwave background photons [38], which is measured to be $\tau = 0.088 \pm 0.015$ by WMAP.

The relationship between the parameters α and T_{vir} can in principle be derived from the hierarchical formation model, although many uncertain astrophysical factors could be involved. Combining such a theoretical relationship with the result presented in this paper, we may obtain a more stringent constraint on the value of T_{vir} as well as the CSFH.

We greatly acknowledge the anonymous referee for his/her valuable comments, which have significantly improved our work. This work is supported by the National Natural Science Foundation of China (grant nos 11103004, 11073008, and 11178001) and by the Self-Determined Research Funds of CCNU from the colleges basic research and operation of MOE of China (Grant Nos. CCNU12A01010).

- 1 Bromm V, et al. The first stars. ARAA, 2004, 42: 79-118
- 2 Glover S. The Formation Of The First Stars In The Universe. Space Science Reviews, 2005, 117: 445-508
- 3 Broom V, Yoshida N, Hernquist L, McKee C F. The formation of the first stars and galaxies. Nature, 2009, 459: 49-54
- 4 Hauser M, et al. The COBE Diffuse Infrared Background Experiment Search for the Cosmic Infrared Background. I. Limits and Detections. ApJ, 1998, 508: 25-43
- 5 Kashlinsky A, et al. Tracing the first stars with fluctuations of the cosmic infrared background. Nature, 2005, 438: 45-50
- 6 Kashlinsky A, et al. ERRATUM: "NEW MEASUREMENTS OF COSMIC INFRARED BACKGROUND FLUCTUATIONS FROM EARLY EPOCHS". ApJL, 2007, 657: L131CL131
- 7 Matsumoto T, et al. Infrared Telescope in Space Observations of the Near-Infrared Extragalactic Background Light. ApJ, 2005, 626: 31-43
- 8 Thompson R I, et al. Constraints on the Cosmic Near-Infrared Background Excess from NICMOS Deep Field Observations. ApJ, 2007, 657: 669-680
- 9 Kashlinsky, A. Cosmic Infrared Background from Population III Stars and Its Effect on Spectra of High- z Gamma-Ray Bursts. ApJ, 2005, 633:L5-L8
- 10 Arendt R G, et al. Cosmic Infrared Background Fluctuations in Deep Spitzer Infrared Array Camera Images: Data Processing and Analysis. The Astrophysical Journal Supplement Series, 2010, 186: 10-47
- 11 Dwek E, Arendt R G & Krennrich F. The Near-Infrared Background: Interplanetary Dust or Primordial Stars? APJ, 2005, 635: 784-794
- 12 Haiman Z. Formation of the first stars and quasars. Advance in Space Research, 1999, 23: 915-924
- 13 Haiman Z. Formation of the First Massive Stars and the Reionization History of the Universe. Baltic Astronomy, 2004, 13: 341-348
- 14 Hopkins A M, Beacom J F. On the Normalization of the Cosmic Star Formation History. ApJ, 2006, 651: 142-154
- 15 Daigne F, Rossi E M, Mochkovitch R. Formation and evolution of compact binaries in globular clusters - I. Binaries with white dwarfs. MNRAS, 2006, 372: 1034-1059
- 16 Bouwens R J, et al. $z \sim 7-10$ Galaxies in the HUDF and GOODS Fields: UV Luminosity Functions. ApJ, 2008, 686: 230-250
- 17 Yüksel H, et al. Revealing the High-Redshift Star Formation Rate with Gamma-Ray Bursts. APJ, 2008, 683: L5-L8
- 18 Kistler M D, et al. The Star Formation Rate in the Reionization Era as Indicated by Gamma-Ray Bursts. ApJ, 2009, 705: L104-L108
- 19 Ishida E E O, de Souza R S, et al. Probing cosmic star formation up to $z=9.4$ with gamma-ray bursts. MNRAS, 2011, 418: 500-504
- 20 Elliott J, et al. Planetary transit candidates in the CoRoT-SRc01 field. A&A, 2012, 539: 14-29
- 21 Aguirre A, et al. Metal Enrichment of the Intergalactic Medium in Cosmological Simulations. ApJ, 2001, 561: 521-549
- 22 Madau P, Ferrara A, Rees M J. Early Metal Enrichment of the Intergalactic Medium by Pregalactic Outflows. ApJ, 2001, 555: 92-105
- 23 Furlanetto S R. METAL ABSORPTION LINES AS PROBES OF THE INTERGALACTIC MEDIUM PRIOR TO THE REIONIZATION EPOCH. ApJ, 2003, 588: 18-34
- 24 Furlanetto S R, Loeb A. IS DOUBLE REIONIZATION PHYSICALLY PLAUSIBLE? ApJ, 2005, 634: 1-13
- 25 Press W H, Schechter P. Formation of galaxies and clusters of galaxies by self-similar gravitational condensation. ApJ, 1974, 187: 425-438
- 26 Barkana R, Loeb A. IN THE BEGINNING: THE FIRST SOURCES OF LIGHT AND THE REIONIZATION OF THE UNIVERSE. Physics Reports, 2001, 349: 125-238
- 27 Eisenstein D J, Hu W. BARYONIC FEATURES IN THE MATTER TRANSFER FUNCTION. ApJ, 1998, 496: 605-314
- 28 Mo H J, White S D M. The abundance of clustering of dark haloes in the standard Λ CDM cosmogony. MNRAS, 2002, 336, 112-118
- 29 Holzbauer L N, et al. Fluctuations in the high-redshift Lyman-Werner and Ly radiation backgrounds. MNRAS, 2012, 419: 718-731
- 30 Abel T. 1995, Ph. D. Thesis, University of Regensburg
- 31 Tegmark M, Silk J, et al. How Small Were the First Cosmological Objects? APJ. 1997, 474: 1-12
- 32 Haiman Z, Abel T, Rees M J. THE RADIATIVE FEEDBACK OF THE FIRST COSMOLOGICAL OBJECTS. APJ, 2000, 534: 11-24
- 33 Ciardi B, Ferrara A, Abel T. INTERGALACTIC H_2 PHOTODISSOCIATION AND THE SOFT ULTRAVIOLET BACKGROUND PRODUCED BY POPULATION III OBJECTS. APJ, 2000, 533: 594-600
- 34 Tumlinson J, Shull J M, Venkatesan A. COSMOLOGICAL EFFECTS OF THE FIRST STARS: EVOLVING SPECTRA OF POPULATION III. APJ, 2003, 584: 608-620
- 35 Schaerer D. On the properties of massive Population III stars and metal-free stellar populations. A&A, 2002, 382: 28-42
- 36 Komatsu E, et al. Seven-year Wilkinson Microwave Anisotropy Probe (WMAP) Observations: Cosmological Interpretation. ApJS, 2011, 192: 18-64
- 37 Bouwens R J, Illingworth G D, Labbe I, et al. A candidate redshift $z \sim 10$ galaxy and rapid changes in that population at an age of 500 Myr. Nature, 2011, 469: 504-507
- 38 Yu, Y. W., et al. 2012, JCAP, accepted